University of Wisconsin-Stevens Point

Student: Nicholas Quisler
Faculty Mentor: Sebastian Zamfir
Department of Physics and Astronomy

Exploring Quasars Through Their Broad Emission Line Shifts and Radio Morphology

Abstract

Quasars are the most energetic types of Active Galactic Nuclei, presumably powered by supermassive black holes accreting matter from their immediate vicinity. Their copious energy output originates in a relatively small volume of space, much smaller than the distance that separates the Sun from its nearest stellar neighbor. Given their cosmological distances and their compact physical size, the only hope to resolve their structure relies on spectroscopy, rather than direct imaging. We investigate large samples of optical quasar spectra, originally acquired by the Sloan Digital Sky Survey and subsequently measured and cataloged by various professional groups. We use very recent, vetted catalogs of spectral measures (publicly available) and also extract their radio morphology maps from databases produced by the Very Large Array of Radio Telescopes at 20 cm wavelength. The main focus is on the shifts (relative to the internal rest-frame of the quasars) of the characteristic broad emission lines (Balmer lines, MgII l2800 Å, etc.) and the extended radio-morphology driven by large-scale jets launched by the active galactic engines. We report on new insights into the fascinating world of quasars using a multi-wavelength approach.

Proposed Model of a Quasar

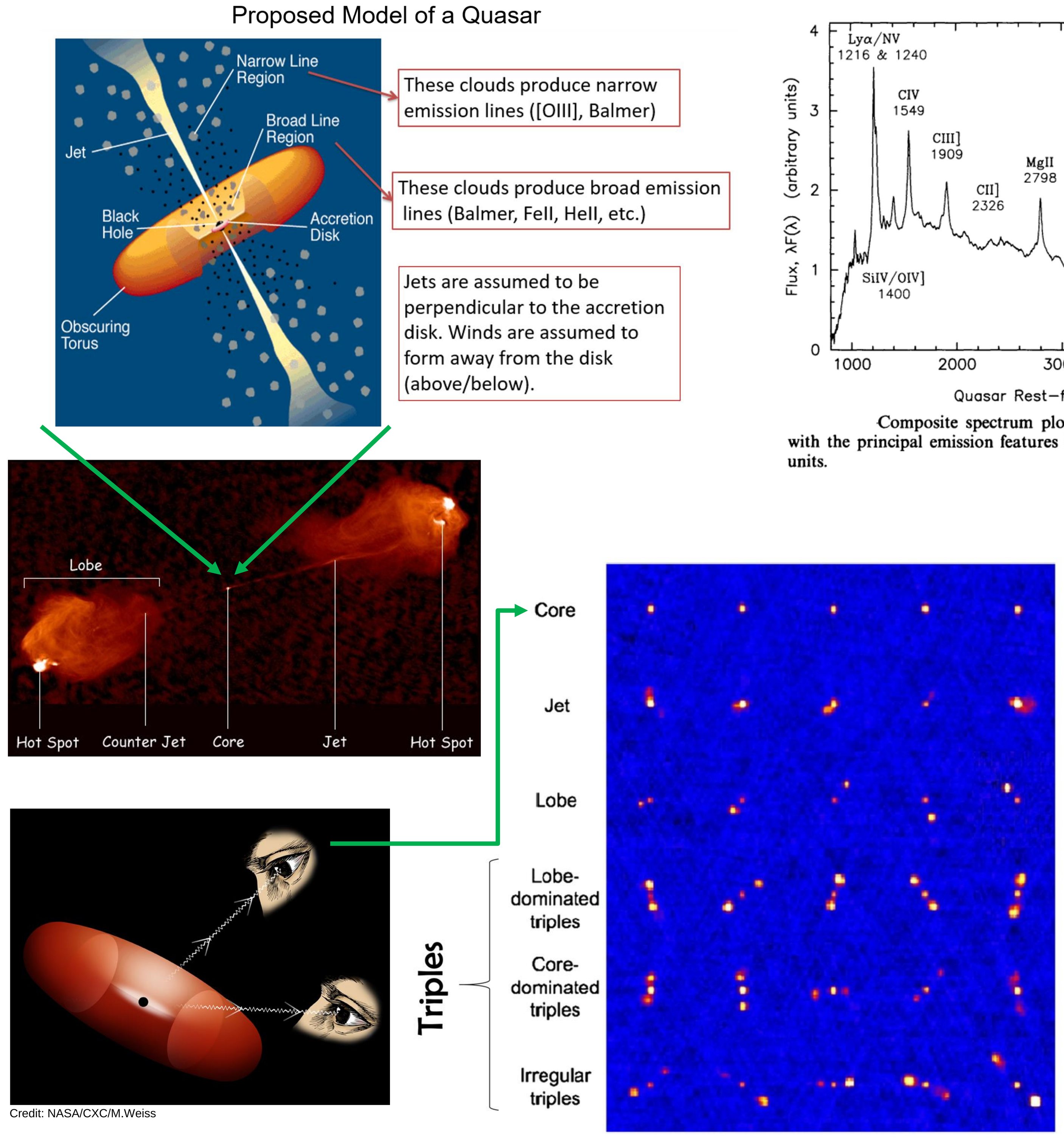

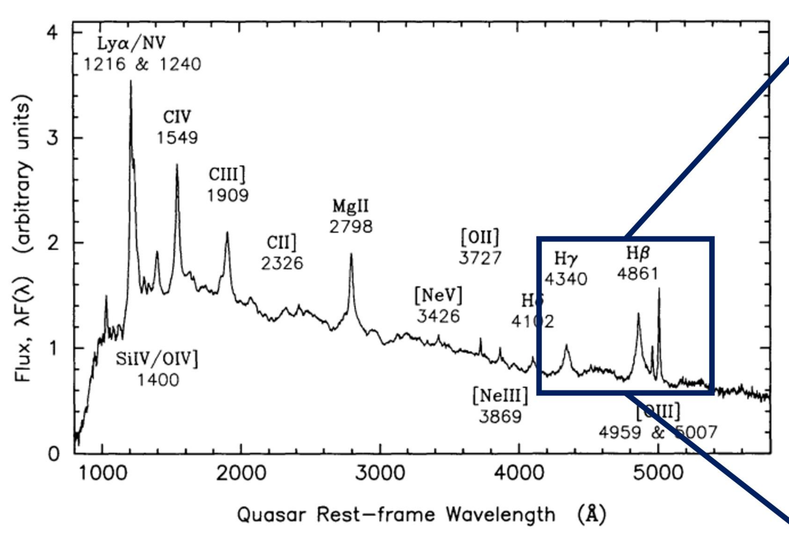

Composite spectrum plotted as λF(λ) vs. rest-frame wavelength with the principal emission features identified. The flux scale is in arbitrary units.

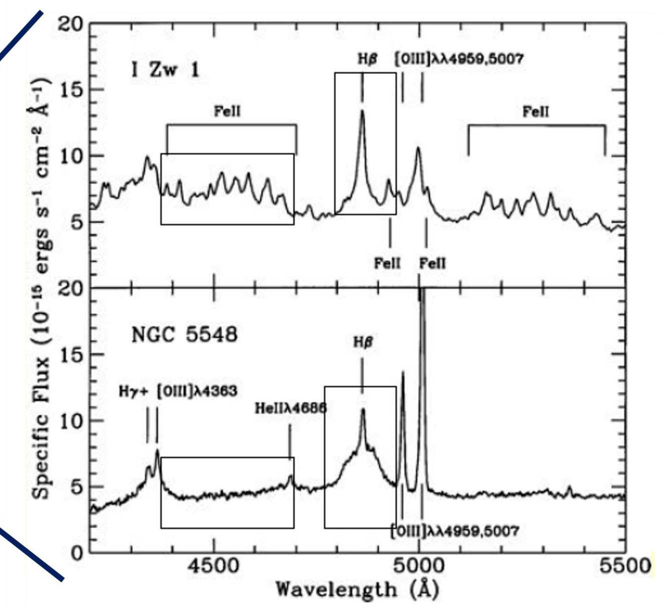

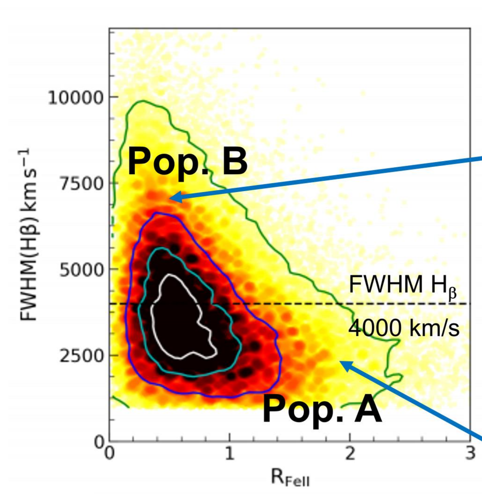

Hβ line width vs. optical Fe II strength. The 20, 40, 68 and 95 percentile density contours along with the density map are shown. The horizontal line at 4000 km s^{-1} is also shown.

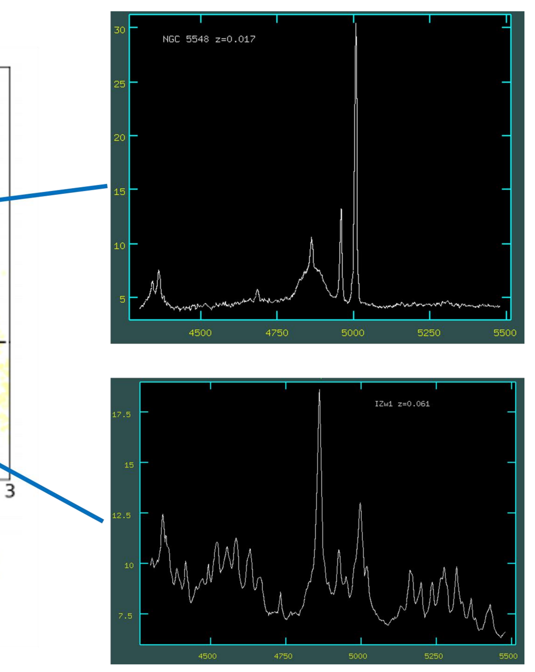

Sample Selection Method

Sample 1

- Calderone 2017's QSFIT with an applied restriction of Hβ (aka Hb) and MgII being present. (N=17,104)
- Cross-Checked with Faint Images of the Radio Sky at Twenty-Centimeters (FIRST) and recorded the flux of the core and lobes (if available). Also classified sources based on their radio maps. (N=1,530)
- Uploaded Rakshit 2020 data and restricted the Signal-to-Noise (S/N) >10. (N=815)
- Uploaded additional data from Paris 2018 to help calculate R (core-to-lobe flux density ratio at 20 cm).
- Used the peak wavelength of various broad lines in conjunction with their vacuum wavelengths to calculate the velocity shifts with respect to the rest frame of the quasar.
- Used only core and triples in Sample 1 plots. (N=619+104=723)

Sample 2

- Rakshit 2020 with an applied restriction of S/N > 20 (N=13,888)
- Used the peak wavelength of various broad lines in conjunction with their vacuum wavelengths to calculate the velocity shifts with respect to the rest frame of the quasar (VOFF).
- Used the Rest-frame Equivalent-Width (EW) of optical FeII complex within the 4435-4685Å and the Rest-frame EW of Hβ broad (BR) component to calculate RFeII (aka RFe).

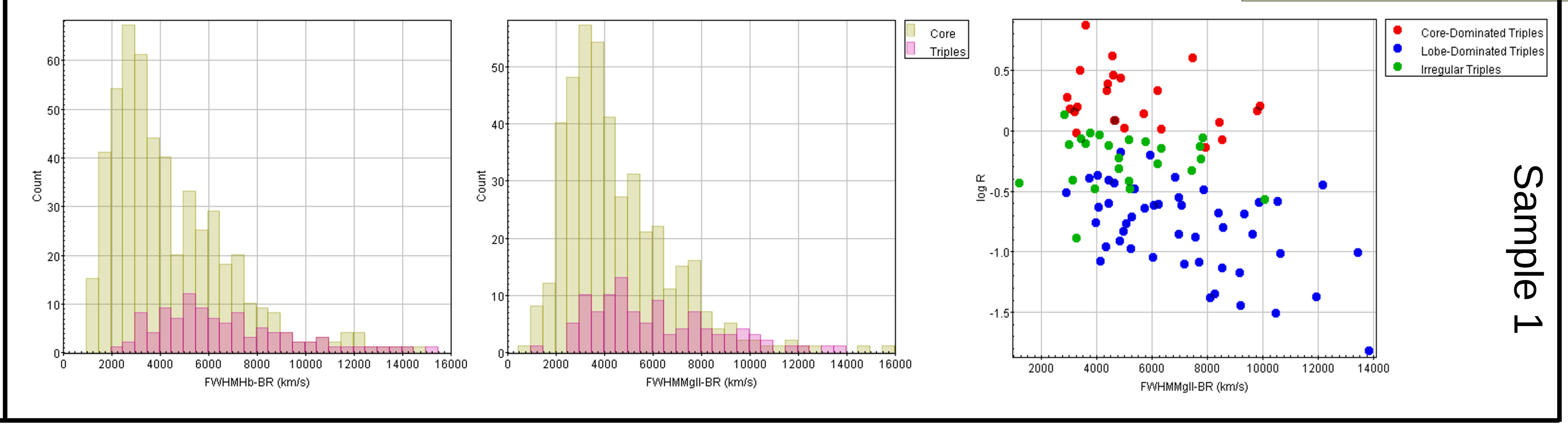

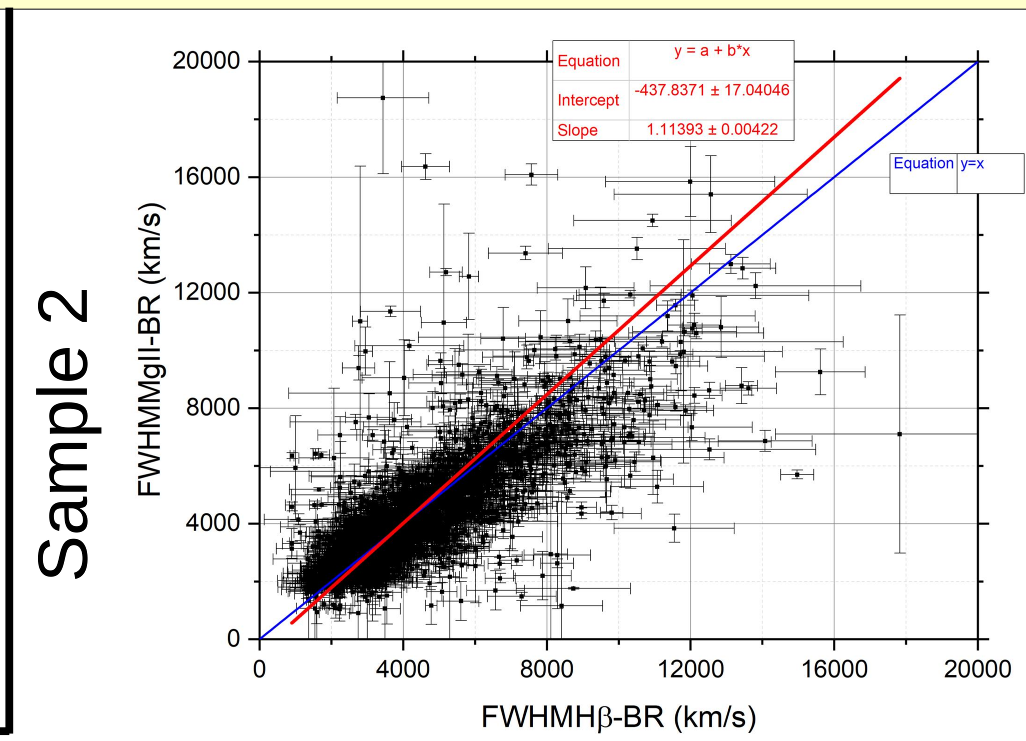

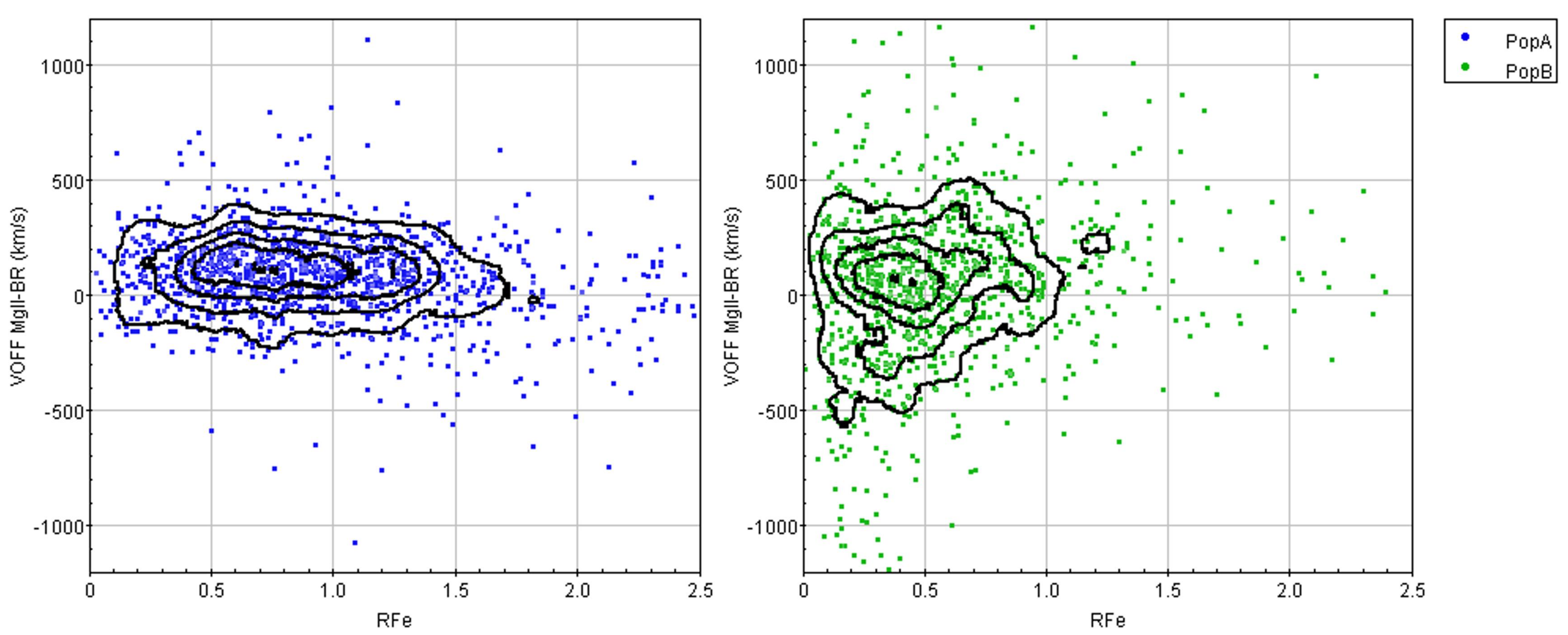

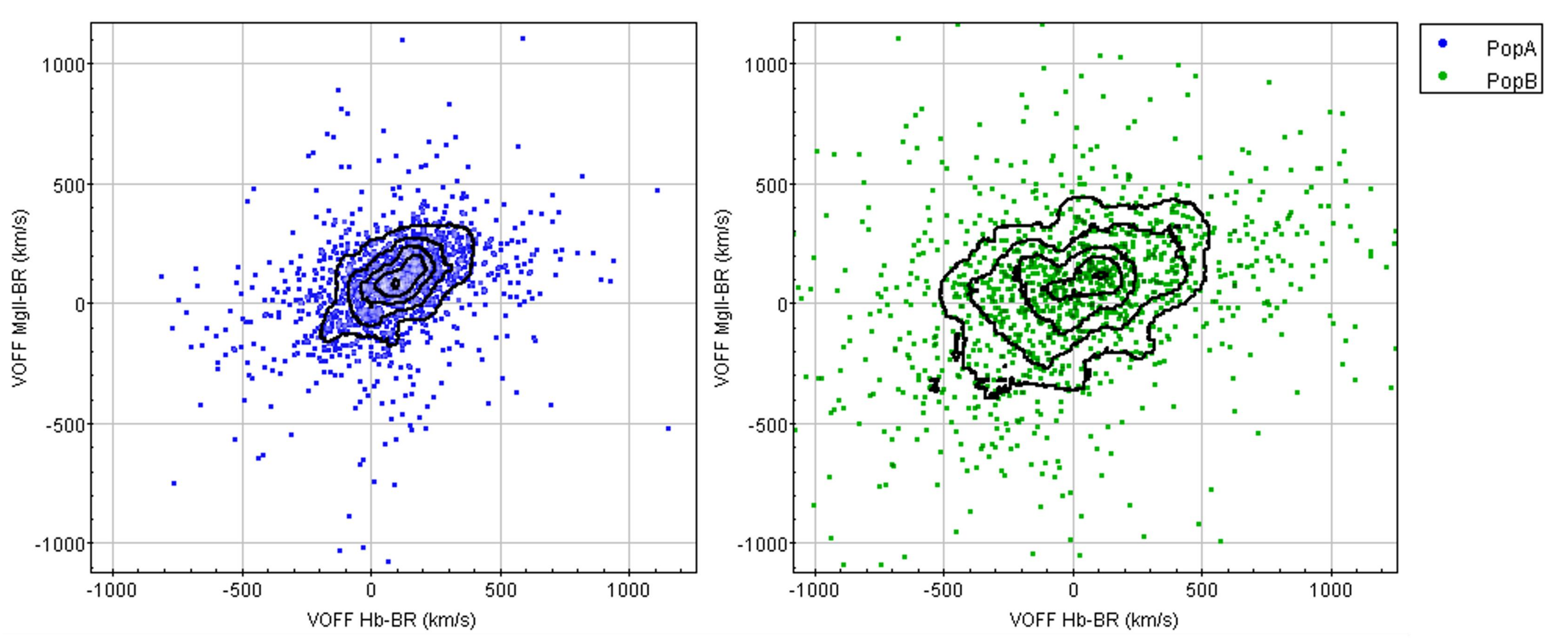

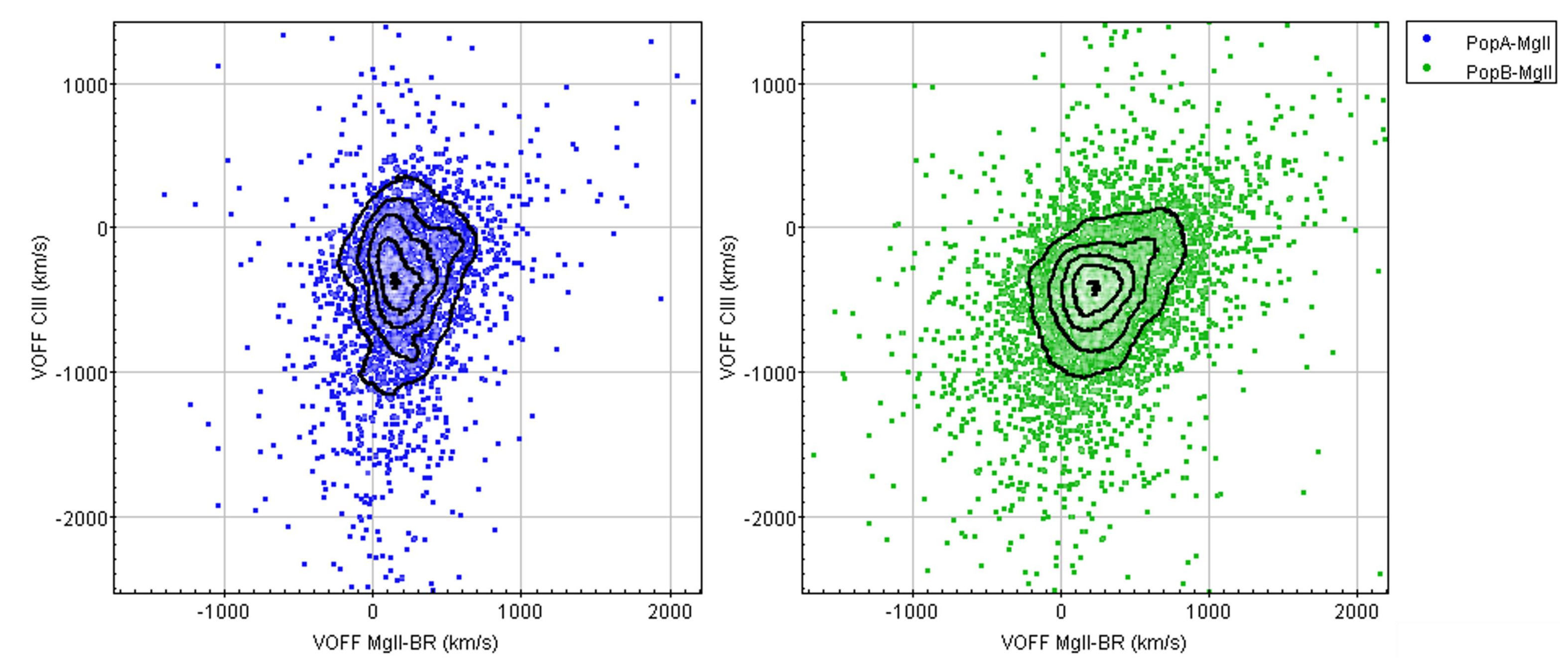

Notable Findings

Sample 1

- If you see the broad line producing clouds from one side, you get less broadening because of the Doppler effect. If you see them with an edge on orientation, you get a broader profile because of the amplified Doppler effect. The two histograms of the FWHM Hβ and MgII broad components seem to be consistent with the hypothesis of orientation. The core-quasars show, on average, narrower profiles in both Hβ and MgII broad lines, which likely come from the same clouds of the quasar. The triples possibly represent more of an edge-on view of the quasar, so we get broader profiles. Some core classified quasars may be triples viewed from a pole-on view.
- There is a relationship between the morphology of the quasar and its core-to-lobe flux density. Wider MgII broad emission lines correspond to lobe-dominated-triples. As MgII broad lines get narrower, our sources are more dominated by irregular triples and core-dominated triples, with the jet axis presumably closer to our line-of-sight.

Sample 2

- The FWHM of the broad MgII correlate well with Hβ, especially at smaller values. This effect may provide hints at two distinct quasar groups, population-A and population-B
- Positive values of MgII seem to prevail most for population-A quasars, meaning the broad emission lines are red-shifted relative to the zero-rest frame of the quasar itself. Population-A quasars contain a wider range of RFe values compared to population-B quasars, which show a tighter spread. This again provides evidence that population-A and population-B quasars show different characteristics, previously seen in the scatterplot of the FWHM of broad Hβ vs RFe.
- A much higher fraction of quasars show red-shifted MgII profiles in population-A. We also have good evidence that MgII and Hβ share similar line shift behavior. Population-A again shows red-shifted emission lines. The contours and the zero lines in both axes show red-shifted dominance. In comparison, population-B shows different, and wider spread line shifts. There is also a more symmetric distribution around the zero line for Hβ, and a slight dominance of redshifts in the MgII lines, setting population-B apart from population-A.
- As we lose Hβ from our spectral window, we get higher redshift quasars with CIII at 1909 Å and MgII at 2798 Å being present. We get different line-shift behavior when we distinguish between the population A-B subsets, only this time instead of basing it on Hβ, we base it on MgII. Since we are talking about broad lines, we naively expect that the same clouds produce these lines. We are trying to stratify information about these clouds to show that different regions in the broad-line emitting clouds exist, which create this systematic effect we see in the line shifts. The internal kinematics tells us a lot about the quasars. In both populations, even more dramatically in population-B, most quasars show a blue-shifted CIII profiling. Population-B quasars and population-A quasars also show red-shifted MgII profiles.

References:

Software: OriginPro, TOPCAT (Taylor 2005)

1) Becker, Robert H., and Richard L. White. "FIRST Catalog Search." *The VLA FIRST Survey*. 17 Dec. 2014. Web.
2) Bridle, Alan. Parts of a DRAGN. Digital image. Double Radio Sources Associated with Galactic Nuclei. NRAO Charlottesville, 28 June 2006. Web. 29 Apr. 2021.
3) Calderone et al., MNRAS, 472, 4051 (2017)
4) Francis, Paul J., et al. "A High Signal-to-Noise Ratio Composite Quasar Spectrum." The Astrophysical Journal, vol. 373, 1991, p. 465, doi:10.1086/170066.
5) Hogg, D. et al. "The K correction." arXiv: Astrophysics (2002): n. pag.
6) Kimball, A. et al. "CORRELATIONS OF QUASAR OPTICAL SPECTRA WITH RADIO MORPHOLOGY." The Astronomical Journal 141 (2011): 182.
7) Pâris, I. et al. "The Sloan Digital Sky Survey Quasar Catalog: Fourteenth data release." Astronomy and Astrophysics 613 (2018): n. pag.
8) Rakshit, S. et al. "Spectral properties of quasars from Sloan Digital Sky Survey data release 14: The catalog." arXiv: Astrophysics of Galaxies (2019): n. pag.
9) Soltis, J. et al. "The Parallax of Omega Centauri Measured from Gaia EDR3 and a Direct, Geometric Calibration of the Tip of the Red Giant Branch and the Hubble Constant." arXiv: Astrophysics of Galaxies (2020): n. pag.
10) Sulentic, J. et al. "VLT/ISAAC spectra of the Hβ region in intermediate-redshift quasars II. Black hole mass and Eddington ratio ,." Astronomy and Astrophysics 456 (2006): 929-939.
11) Taylor, M.. "TOPCAT & STIL: Starlink Table/VOTable Processing Software." (2005).
12) OriginPro, Version 2021. OriginLab Corporation, Northampton, MA, USA.
13) Urry, M. & Padovani, P. 1995, Publications of the Astronomical Society of the Pacific, Volume 107, p.803

Acknowledgements:
This project was funded in part by a grant through the Wisconsin Space Grant Consortium (WSGC; awarded to Nicholas Quisler).